was necessary in order to find the delay setting to satisfy this condition. The output of the optical circuit was observed on a 50GHz oscilloscope with a 35GHz photodiode or an RF spectrum analyser.

Results and discussion: Fig. 2 shows oscilloscope traces of the input pulse train at 10GHz, and the output at 5GHz, showing clearly the divide by two functionality. Fig. 3 shows the input at 20GHz and the output at 10GHz. A microwave spectrum analyser trace for the 20GHz input and the output is shown in Fig. 4. Similar spectra were measured at 10GHz. As has been discussed elsewhere [8], clock division occurs because the initial pulse in the switching pulse train encounters an unsaturated SOA, and causes a large phase change. The lifetime of the SOA prevents full recovery of the gain, and so subsequent pulses pass through a saturated SOA and cause smaller and approximately equal phase shifts. The differential phase shift of the initial pulse compared to the rest is retained by the system due to the feedback, and after many round trips, clock division is observed as a stable output. According to our modelling [8], clock division occurs when the product of the SOA lifetime and the repetition rate is approximately between 0.6 and 1.2. Measurements indicate an SOA lifetime of ~70ps at typical operating currents of 300mA, which would predict clock division between ~10 and 18GHz, in reasonable agreement with observation.

Conclusions: We have experimentally demonstrated all-optical clock division at 10 and 20GHz using a circulating shift register architecture with a short lifetime SOA. These results clearly demonstrate the scaleability of this clock division technique to much higher repetition rates.

27 April 1998
Electronics Letters Online No: 19980948

A.E. Kelly, R.J. Manning, A.J. Poustie and K.J. Blow (*BT Laboratories, Martlasham Heath, Ipswich, Suffolk, IP5 3RE, United Kingdom*)

E-mail: tony.kelly@bt-sys.bt.co.uk

References

1 MANNING, R.J., ELLIS, A.D., POUSTIE, A.J., and BLOW, K.J.: 'Semiconductor laser amplifiers for ultrafast all-optical signal processing', *J. Opt. Soc. Am. B*, 1997, **14**, pp. 3204–3216

2 HESS, R., CARACCIA-GROSS, M., VOGT, W., GAMOER, E., BESSE, P.A., DUELK, M., GINI, E., MELCHIOR, H., MIKKELSEN, B., VAA, M., JEPSEN, K.E., STUBJKAER, K.E., and BOUCHOULE, S.: 'All-optical demultiplexing of 80 to 10Gb/s signals with monolithic integrated high performance Mach-Zehnder interferometer', *IEEE Photonics. Technol. Lett.*, 1998, **10**, pp. 165–167

3 SOKOLOFF, J.P., PRUCNAL, P.R., GLESK, I., and KANE, M.: 'A terahertz optical asymmetric demultiplexer (TOAD)', *IEEE Photonics Technol. Lett.*, 1993, **5**, pp. 787–790

4 POUSTIE, A.J., BLOW, K.J., and MANNING, R.J.: 'All-optical regenerative memory for long term data storage', *Opt. Commun.*, 1997, **140**, pp. 184–186

5 POUSTIE, A.J., MANNING, R.J., and BLOW, K.J.: 'All-optical circulating shift register using a semiconductor optical amplifier in a fibre loop mirror', *Electron. Lett.*, 1996, **32**, pp. 1215–1216

6 HALL, K.L., DONNELLY, J.P., GROVES, S.H., FENNELLY, C.I., BAILEY, R.J., and NAPOLEONE, A.: '40Gbit/s all-optical circulating shift register with an inverter', *Opt. Lett.*, 1997, **22**, pp. 1479–1481

7 MANNING, R.J., POUSTIE, A.J., and BLOW, K.J.: 'All-optical clock division using a semiconductor optical amplifier loop mirror with feedback', *Electron. Lett.*, 1996, **32**, pp. 1504–1506

8 BLOW, K.J., MANNING, R.J., and POUSTIE, A.J.: 'Nonlinear optical loop mirrors with feed back and a slow nonlinearity', *Opt. Commun.*, 1997, **134**, pp. 43–48

9 KELLY, A.E., MARCENAC, D.D., and NESSET, D.: '40Gbit/s wavelength conversion over 24.6nm using FWM in a semiconductor optical amplifier with an optimised MQW active region', *Electron. Lett.*, 1997, **33**, pp. 2123–2124

10 MARCENAC, D.D., ELLIS, A.D., and MOODIE, D.G.: '80Gbit/s using electroabsorption modulators', *Electron. Lett.*, 1998, **34**, pp. 101–103

Locally-pumped repeatered and remotely-pumped repeaterless 1.55μm CATV video lightwave systems over 127km standard singlemode fibre

S.L. Tzeng, C.H. Chang and Y.K. Chen

1.55μm 80 channel AM CATV video lightwave systems are investigated using 1480nm locally- and remotely-pumped amplified techniques for the first time. Satisfactory CNR performances of 45dB with CSO/CTB of 61/70dB are achieved for a locally-pumped repeatered system over a standard 127km singlemode fibre. Based on the repeatered technique, system design and operation considerations of the remotely-pumped repeaterless system are also discussed. Repeaterless systems may find important applications for inter-islands and island-hopping with no active components allowed.

Introduction: Recently, 1.55μm CATV systems using externally-modulated transmitters (EM-TXs) and cascaded erbium-doped fibre amplifiers (EDFAs) have been studied extensively [1 – 4] to provide supertrunk applications. The EDFAs used are all 980nm-pumped due to the inherently low noise-figure (NF) characteristic, to obtain a better carrier-to-noise ratio (CNR). However, it is infeasible to have in-line amplifiers for many applications such as inter-islands, island hopping, and some intracity links. Therefore, remote amplification or repeaterless transmission with no active components included in the system links is required. The 980nm pumping technique cannot be used for remote pumping because of its high attenuation of 1.15dB/km of standard singlemode fibre (SMF). Fortunately, 1480nm pumping is suitable for remote pumping because of its low transmission loss of 0.24dB/km and the availability of 1.48μm high-power (1.3W) optical pump sources [5]. Repeaterless digital telecommunication systems including remote pumping of EDFAs in conjunction with Raman amplification have been demonstrated and deployed [6]. However, 1480nm-pumped repeatered and repeaterless techniques for CATV lightwave systems have not yet been reported. In this Letter, we investigate both 1480nm locally-pumped repeatered and remotely-pumped repeaterless CATV systems, to the best of our knowledge for the first time. Satisfactory performances of CNR with composite second-order (CSO) and composite triple beat (CTB) are achieved for the locally-pumped repeatered system. Extending this technology, system design and operation considerations of the remotely-pumped repeaterless CATV system are investigated.

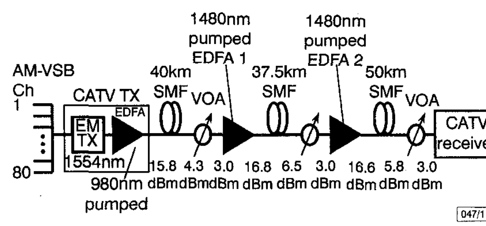

Fig. 1 *1480nm locally-pumped EDFA-repeatered CATV transmission system*

Demonstration of locally-pumped repeatered system: Fig. 1 shows the 1480nm locally-pumped repeatered CATV system. The EX-TX at 1554nm carries an 80 channel NTSC AM-VSB video signal, provided by a multiple-carrier generator, which is amplified by a 980nm-pumped EDFA with an output power of 16dBm and NF = 4.8dB. The optical modulation index of EM-TX is ~3.5% and its stimulated Brillouin scattering (SBS) suppression capability is ~16.5dBm. Each in-line amplifier, employing a bi-directionally dual-pumping scheme, consists of two 1480nm pump-laser diodes, two 1.48/1.55μm WDM couplers, a piece of EDF, and an optical isolator. Each pump laser has an output power of ~75mW, and an EDF (Lucent MP980) with an optimum length of 20m is used. Two in-line amplifiers (EDFA1 and EDFA2) have the same output power of ~16.6dBm. The NF of EDFA1 and EDFA2 is ~6.5 and 6.9dB, respectively. Three variable optical attenuators (VOAs) are used to control the launched input power of the in-line EDFAs to be 3dBm. The evolution of EX-TX signal power levels in the 127.5km SMF link is depicted in Fig. 1. The input power of the receiver was kept at 3dBm.

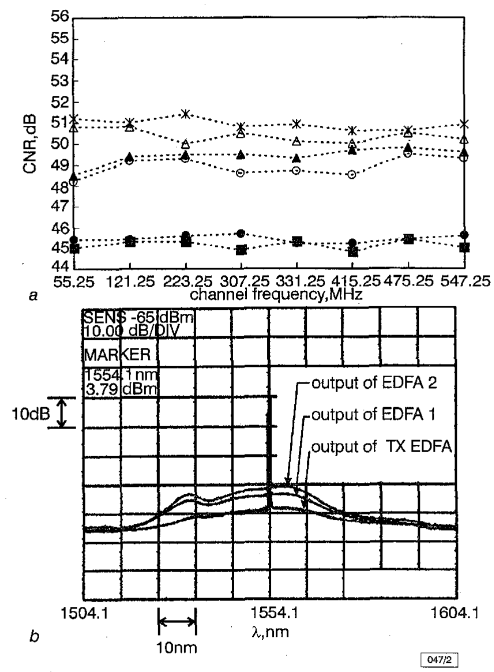

Fig. 2 *Evolution of system CNR and amplified spontaneous emission in locally-pumped repeatered CATV system*

a System CNR
✳ B – B
▲ 40 km + EDFA
● 77.5 km + EDFA
△ 40 km
O 77.5 km
■ 127.5km
b Amplified spontaneous emission
RB = 0.1nm

Fig. 2*a* shows the evolution of the measured CNR against channel frequencies. The averaged CNR after the 127.5 km link is ~45dB, which is ~6dB lower than the back-to-back (B-B) case. This degradation is attributed to the high NF of in-line EDFAs (which degrades the relative intensity noise) and the high signal-spontaneous (s-sp) and spontaneous-spontaneous (sp-sp) beat noises, which resulted from the accumulated amplified spontaneous emission (ASE) noise of the cascaded amplifiers. The accumulated ASE peak power level at the output port of EDFA2 has increased to ten times that generated by the transmitter EDFA, as shown in Fig. 2*b*. The evolutions of CSO and CTB were also measured in detail. The worst system CSO at high-frequency channels was 61dB. The CSO degradation of 6–10dB, as compared with the B-B case, is attributed to the interaction of the self-phase modulation effect and fibre chromatic dispersion [2]. The worst system CTB was 70dB. These CNR and CSO/CTB performances still meet most supertrunk systems.

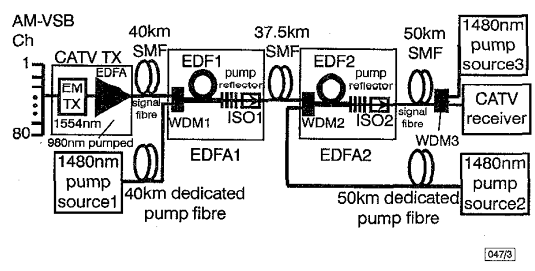

Fig. 3 *1480nm remotely-pumped repeaterless CATV transmission system*

Design of remotely-pumped repeaterless system: Fig. 3 shows the proposed 1480nm remotely-pumped repeaterless CATV system. No pump laser diodes and active components are used in the in-line EDFAs. Remote amplification can be realised by the following pumping methods: (i) via the signal fibre to a remote EDF, (ii) via a dedicated pump fibre to a remote EDF, (iii) via the signal fibre for pure Raman amplification, and (iv) by combining (ii) and (iii). Of these, method (iv) has shown the best power budget improvement in telecommunication systems, and method (ii) has also shown good capability [6]. Pure silica-core fibre is assumed as the dedicated pump fibre due to its lower background loss. The UV-induced 1480nm fibre Bragg grating pump reflector, with reflectivity = 99% and FWHM = 20nm, is used to reflect the residual pump power into the EDF to increase the pump efficiency. The isolators (ISO1, ISO2) are employed to eliminate Rayleigh backscatters. The input signal power of EDFA1 and EDFA2 should be kept to > 0dBm to maintain high CNR. The optimum location of remote EDF is determined by the interplay of fibre nonlinearities (SBS and stimulated Raman scattering, SRS) and the power conversion efficiency of EDFA.

To achieve the same system performances as the locally-pumped system, pumping methods (ii) and (iv), both in forward pumping schemes for realising low NF characteristics, are adopted for EDFA1 and EDFA2, respectively, in the repeaterless CATV system. The 1480nm pump source 1 requires 1.3W to provide 142mW of launched pump power into the remote EDF1 to offer 16dBm output power. If we apply method (ii) on EDFA2, then pump source 2 requires 2.3W to offer 16dBm of output power. However, this pump power is harmful to the system because it may exceed the SRS threshold. Therefore, in addition to pumping remote EDF2 via the dedicated fibre using pump source 2 with 1.3W, pumping the signal fibre through Raman amplification by using an additional pump source 3 with 1.3W is required for EDFA2. In this system, any Stokes emission at 1.55μm, generated from the high-power 1480nm pump in the dedicated pump fibre, will not interfere with the CATV signal due to the filtering operation of the WDM1 and WDM2 couplers. The CNR can be further improved by using a 1 nm optical bandpass filter located immediately after each in-line EDFA to filter out most of the ASE power and thus drastically decrease the sp-sp and s-sp beat noises.

Conclusions: We have demonstrated the 1480nm locally-pumped EDFA-repeatered CATV system over a standard SMF of 127.5km. A CNR of 45dB with CSO/CTB of ~61/70dB has been obtained. We have also investigated the repeaterless system using remotely-pumped EDFAs and Raman amplification. System design and operation considerations have been described. The repeaterless CATV system may find important applications for inter-islands and island-hopping.

Acknowledgments: We are grateful to W.Y. Guo for the loan of CATV transmitter and Jing-Hong Su for technical assistance.

20 April 1998
Electronics Letters Online No: 19980924

S.L. Tzeng (*Department of Electrical Engineering, National Taiwan University, Taiwan, Republic of China*)

C.H. Chang and Y.K. Chen (*Institute of Electro-Optical Engineering, National Sun Yat-Sen University, PO Box 59-83, Kaohsiung, Taiwan, Republic of China*)

Y.K. Chen: Corresponding author

E-mail: ykchen@mail.nsysu.edu.tw

S.L. Tzeng: Also with Chunghwa Telecom Laboratory, Taiwan

References

1 PHILLIPS, M.R.: 'Amplified 1550-nm CATV lightwave systems'. Tech. Dig. 1998 Optical Fiber Communication (OFC'98), 1998, Invited paper TuO3

2 KUO, C.Y., PIEHLER, D., GALL, C., KLEEFELD, A., NILSSON, J., and MIDDLETON, D.L.: 'High-performance optically amplified 1550-nm lightwave AM-VSB CATV transport system'. Tech. Dig. 1996 Optical Fiber Communication (OFC'96), 1996, Paper WN2

3 DAI, H., OVADIA, S., and LIN, C.: 'Hybrid AM-VSB/M-QAM multichannel video transmission over 120km of standard single-mode fiber with cascaded erbium-doped fiber amplifiers', *IEEE Photonics Technol. Lett.*, 1996, **8**, pp. 1713–1715

4 CHEN, Y.K., LIU, Y.L., and LEE, C.C.: 'Directly modulated 1.55μm AM-VSB video EDFA-repeatered supertrunking system over a 110km standard singlemode fibre using split-band and wavelength-division-multiplexing techniques', *Electron. Lett.*, 1997, **33**, pp. 1400–1401

5 GRUBB, S.G., STRASSER, T.A., CHEUNG, W.Y., REED, W.A., MIZRAHI, V., ERDOGAN, T., LEMAIRE, P.J., VENGSARKAR, A.M., and DIGIOVANNI, D.J.: 'High-power 1.48μm cascaded Raman laser in germanosilicate fibres'. Proc. Optical Amplifiers and Their Applications, June 1995, pp. 197–199

6 HANSEN, P.B., and ESKILDSEN, L.: 'Remote amplification in repeaterless transmission systems', *Opt. Fiber Technol.*, 1997, **3**, pp. 221–237

Low optical interchannel crosstalk, fast switching speed, polarisation independent 2 × 2 fibre optic switch using ferroelectric liquid crystals

N.A. Riza and S. Yuan

A novel < –34.13dB optical interchannel crosstalk, 35.3μs switching speed, polarisation independent, reversible 2 × 2 fibre optic switch is demonstrated using four ferroelectric liquid crystal 90° polarisation rotators sandwiched between cube polarisation beam splitters and combiners that also act as crosstalk rejection filters. Applications of the switch include multiwavelength add-drop routing.

Introduction: Recent progress in fibre communications has led to the development of a reconfigurable transparent all-optical network which requires a low loss, high isolation, fast switching speed, reliable, and low cost fibre optic switch, both for singlemode and multimode fibres [1]. Today, the most mature commercially available fibre optic switch is based on opto-mechanical movement [2] and has the advantages of polarisation independence, low loss, and high interchannel isolation. Nevertheless, for large scale network switching, these opto-mechanical switches have limitations such as low scalability, reliability issues due to physically moving parts, and, in most cases, relatively slow switching time (~10–25ms) [3, 4]. Hence, it would be highly desirable to develop a fibre optic switch that maintains to a large degree the key attributes of an opto-mechanical switch but also alleviates most of its limitations. This Letter describes such a switch using ferroelectric liquid crystal (FLC) planar polarisation control technology.

Previously, liquid crystal fibre optic switch research has concentrated on nematic liquid crystal (NLC) devices, resulting in low (< –35dB) crosstalk devices, although at a limited switching speed performance in the millisecond domain [5 – 8]. Recently, we have demonstrated the fast 35μsec switching speed operation of FLC polarisation switches for the 1300nm band typical in analogue fibre optic system applications [9]. Hence, in this Letter we demonstrate the combination of high-speed FLC polarisation rotation technology with other bulk and fibre optics to realise a high performance fibre optic switch that has the key properties of polarisation independence and low crosstalk operation required in fibre optic networks.

Structure: The structure of our 2 × 2 fibre optic switch is shown in Fig. 1. A unique feature of this structure, which is critical for achieving low interchannel crosstalk, is the proper positioning and use of not only the FLC devices but also the cube polarisation optics that work together to reject unwanted switch noise out of the system. For a 2 × 2 switch, there are two states: straight state and exchanging state. To change states in our 2 × 2 switch, four 90° FLC polarisation switches (PS1-PS4) are used. Two pairs of fibre collimators are used as the two inputs and two outputs. The other optical elements include four polarisation beam splitters (PBS1-PBS4), two quarter waveplates (QWPs), two half waveplates (HWPs), two mirrors, and two total internal reflectors (TIRs). The system is in fact a combination of two polarisation dependent switching channels that form a polarisation independent design where one channel is for vertical *s*-polarised light, i.e. the *s*-polarisation channel, and the other channel is for horizontal *p*-polarised light, i.e. the *p*-polarisation channel, as shown in Fig. 1. PBS1 is used to divide the light beam from input fibres 1 and 2 into two orthogonally linearly polarised beams, i.e. the *s*-polarised beam and the *p*-polarised beam. The *s*-polarised beam goes to the *s*-polarisation channel and the *p*-polarised beam goes to the *p*-polarisation channel. The input and output light polarisations of the *s*-polarisation channel are always *s*-polarised, whereas those of the *p*-polarisation channel are always *p*-polarised.

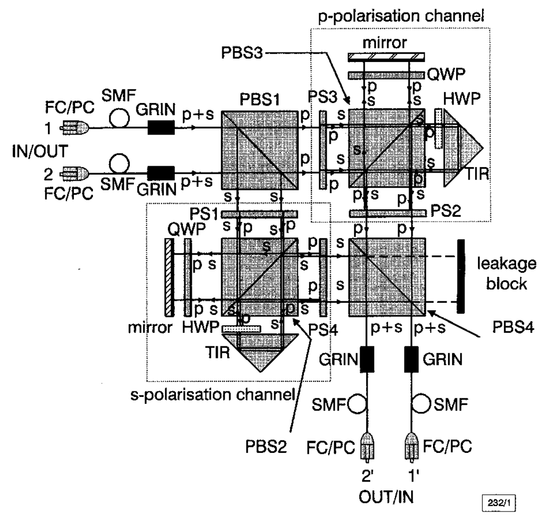

Fig. 1 *Proposed structure of low crosstalk, polarisation independent, 2 × 2 fibre optic switch using FLC devices*

FC/PC: FC/PC connector
SMF: singlemode fibre
p: horizontal polarisation direction
s: vertical polarisation director
GRIN: gradient index lens
QWP, quarter wave plate
HWP: half wave plate
TIR: total internal reflection prism
PS: FLC polarisation switch

For the *s*-polarisation channel, when PS1 is off and PS4 is on, the channel performs in the switch straight state mode. The *s*-polarised beams from nodes 1 and 2 go through PS1 (off) without changing their polarisation directions, and are reflected by PBS2. After passing through the QWP, being reflected by the mirror, and passing through the QWP again, the *s*-polarised light changes to *p*-polarised light that goes through the PBS2 and is changed back to *s*-polarisation by PS4 (on). The *s*-polarised light beams are reflected by PBS4 and finally reach the corresponding output fibres 1′ and 2′. When PS1 is on and PS4 is off, the switch performs the exchanging operation. The polarisation directions of the *s*-polarised beams from the input nodes 1 and 2 are changed to *p*-polarisation by PS1 (on) and then go through PBS2. After passing through the TIR, the beams from nodes 1 and 2 exchange their positions. Since the beams both go through an HWP, they change their polarisation from *p* to *s*-polarisation again. Then both beams are reflected by the PBS2, go through the PS4 (off), and are reflected by PBS4 (which works as a *s*-polariser), before finally reaching their exchanged output nodes, which are output fibres 2′ and 1′, respectively. The switch *p*-polarisation channel is based on the same principle, i.e. when PS3 is on and PS2 is off, the channel performs in the straight state; when PS3 is off and PS2 is on, the channel performs in the exchanging state.

Note that the function of PBS4 is twofold. First, it works as a beam combiner to combine the two signals from both the *s*- and *p*-polarisation channels of the switch, thus coupling the combined *p* and *s* light beams into the output graded index (GRIN) fibre collimators. Secondly, PBS4 works as an interchannel crosstalk suppressor, i.e. it cleans up the beams coupled into the output GRIN fibre collimators and lets the unwanted crosstalk go through to the leakage block. Thus, by using this structure, we can greatly suppress the interchannel and within-channel leakage that arises from imperfect polarisation optics such as FLC devices and cube PBSs.